

In Utero Exposure to TCDD Alters Wnt Signaling During Mouse Prostate Development: Linking Ventral Prostate Agenesis to Downregulated β -Catenin Signaling

Andrew J. Schneider*, Robert W. Moore*, Amanda M. Branam*, Lisa L. Abler[†], Kimberly P. Keil[†], Vatsal Mehta[†], Chad M. Vezina[†], and Richard E. Peterson*,¹

*School of Pharmacy, University of Wisconsin, Madison, Wisconsin 53705 and [†]School of Veterinary Medicine, University of Wisconsin, Madison, Wisconsin 53706

¹To whom correspondence should be addressed. Fax: (608) 262-5345. E-mail: repeterson@pharmacy.wisc.edu.

ABSTRACT

In utero exposure to 2,3,7,8-tetrachlorodibenzo-*p*-dioxin (TCDD) causes ventral prostate agenesis in C57BL/6J mice by preventing ventral prostatic budding in the embryonic urogenital sinus (UGS). TCDD (5 μ g/kg, po) administered to pregnant dams on embryonic day 15.5 (E15.5) activates the aryl hydrocarbon receptor in the UGS mesenchyme, disrupting the mesenchymally derived paracrine signaling that instructs epithelial prostatic budding. How TCDD alters the mesenchymal milieu is not well understood. We previously showed that TCDD disrupts some aspects of Wnt signaling in UGSs grown *in vitro*. Here we provide the first comprehensive, *in vivo* characterization of Wnt signaling in male E16.5 UGSs during normal development, and after *in utero* TCDD exposure. Vehicle- and TCDD-exposed UGSs were probed by *in situ* hybridization to assess relative abundance and localization of RNA from 46 genes that regulate Wnt signaling. TCDD altered the staining pattern of five genes, increasing staining for *Wnt10a* and *Wnt16* and decreasing staining for *Ror2*, *Rspo2*, and *Wif1*. We also used immunohistochemistry to show, for the first time, activation of β -catenin (CTNNB1) signaling in ventral basal epithelium of control UGSs at E16.5. This onset of CTNNB1 signaling occurred immediately prior to the initiation of ventral prostatic budding and is characterized by a pronounced increase in CTNNB1 nuclear localization and subsequent expression of the CTNNB1 signaling target gene, *Lef1*. *In utero* TCDD exposure prevented the onset of CTNNB1 signaling and LEF1 expression in the ventral basal epithelium, thereby elucidating a likely mechanism by which TCDD contributes to failed prostatic budding in the ventral UGS.

Key words: TCDD; Wnt; CTNNB1; mouse; prostate; development

Mouse prostate develops from the fetal urogenital sinus (UGS). Testicular androgens trigger production of paracrine signals in UGS mesenchyme that stimulate the formation of prostate duct progenitors (prostatic buds) from UGS epithelium (reviewed in Cunha, 2008; Thomson, 2008). Prostatic buds are specified in a precise pattern about the caudocranial and dorsoventral axes of the UGS creating anterior, dorsal, lateral, and ventral budding regions. Bud initiation and elongation occurs first in the anterior and dorsal regions beginning around embryonic day

16.5 (E16.5) and last in the lateral and ventral regions beginning around E17.5 (Lin et al., 2003).

2,3,7,8-tetrachlorodibenzo-*p*-dioxin (TCDD), the prototypical aryl hydrocarbon receptor (AHR) agonist, is a persistent, global environmental contaminant that has been shown in toxicity studies to be a carcinogen, immunomodulator, endocrine disruptor, epigenetic modifier, and teratogen (Birnbaum and Fenton, 2003; Couture et al., 1990; Craig et al., 2011; Kerkvliet, 2009; King-Heiden et al., 2012; Knerr and Schrenk, 2006; Leng et al.,

2014; Manikkam et al., 2012; Martinez et al., 2003; Sulentic and Kaminski, 2011; Tian, 2009). *In utero* exposure to TCDD can adversely affect the development of multiple organs and tissues in rodents, including prostate development (reviewed in Vezina et al., 2009). A single dose of TCDD (5 µg/kg) given to pregnant (E13.5–E15.5) C57BL/6J mice inhibits prostatic budding initiation, causing reduced numbers of dorsolateral prostatic buds and a complete lack of ventral prostatic buds (Lin et al., 2003; Vezina et al., 2008). TCDD inhibits budding by activating AHR in the UGS mesenchyme (Ko et al., 2004a). Though UGS mesenchyme is where androgens and TCDD act to promote or inhibit prostatic budding, respectively, TCDD does not seem to inhibit budding by directly downregulating androgen signaling (Ko et al., 2004b). Therefore, we hypothesized that TCDD alters mesenchymally derived paracrine signaling such that either the epithelium does not receive appropriate signals to initiate budding, or it receives signals that actively block budding. We previously studied the effects of TCDD exposure on selected members of the Egf, Fgf, Tgf, and Wnt paracrine signaling pathways (Abbott et al., 2003; Allgeier et al., 2008; Branam et al., 2013; Vezina et al., 2010). Multiple components of the Wnt signaling pathway were dysregulated in UGSs cultured *in vitro* with TCDD. Therefore, we aimed to confirm these findings *in vivo* and assess additional Wnt signaling components to identify TCDD-affected genes that could inhibit prostatic budding.

Wnt signaling is comprised of multiple intracellular signaling cascades that affect diverse cellular responses including transcription, proliferation, differentiation, and migration (Kharraishvili et al., 2011; Nishita et al., 2010; Simons et al., 2012). The Wnt/β-catenin signaling cascade is a major component of Wnt signaling. When activated, β-catenin (CTNNB1), which is degraded under resting conditions, accumulates within the cell, translocates into the nucleus, and activates transcription of target genes. Inhibitors of the Wnt/CTNNB1 signaling cascade, or conditional *Ctnnb1* knockout, impair prostatic budding (Branam et al., 2013; Francis et al., 2013; Mehta et al., 2013; Simons et al., 2012). UGSs cultured *in vitro* with TCDD show reduced expression of CTNNB1 signaling target genes and fewer prostatic buds compared with control UGSs (Branam et al., 2013). Furthermore, AHR activation can downregulate CTNNB1 signaling (demonstrated by reduced CTNNB1 target gene expression) in other rodent tissues and cell types (Kawajiri et al., 2009; Procházková et al., 2011). Thus, CTNNB1 signaling is required for prostatic budding in mice, and AHR activation can downregulate CTNNB1 signaling.

Our previous *in vitro* study revealed that TCDD dysregulates Wnt signaling in the UGS; however, it focused on a limited number of genes. The present study is the first comprehensive *in vivo* evaluation of Wnt signaling activity in UGSs from E16.5 C57BL/6J male mice. At E16.5, some anterior and dorsal buds have formed, but lateral and ventral bud initiation has not yet occurred. Because TCDD exposure prevents ventral budding, we investigated how TCDD affects Wnt signaling in the ventral UGS prior to bud formation. We used *in situ* hybridization (ISH) to characterize the relative abundance and localization of RNAs from 46 Wnt pathway genes during both normal development and after exposure to TCDD. TCDD increased staining of wingless-related MMTV integration site 10a (*Wnt10a*) and *Wnt16* and decreased staining of receptor tyrosine kinase-like orphan receptor 2 (*Ror2*), R-spondin2 (*Rspo2*), and Wnt inhibitory factor 1 (*Wif1*). In addition to this broad survey of Wnt signaling, we investigated CTNNB1 signaling in the UGS in detail. This is the first report to show activation of CTNNB1 signaling immediately prior to budding initiation in basal epithelial cells during normal prostate develop-

ment. Immunohistochemistry (IHC) revealed that CTNNB1 accumulates intracellularly and translocates to the nucleus where it induces expression of known target genes Lymphoid enhancer binding factor 1 (*Lef1*) and *Wif1*, as well as putative target gene *Ror2*. *In utero* TCDD exposure blocks activation of CTNNB1 signaling in the ventral UGS. CTNNB1 fails to accumulate and, correspondingly, there is a pronounced reduction in target gene expression in ventral basal epithelium. This block in activation of CTNNB1 signaling is likely a key mechanism by which TCDD causes budding failure in the ventral UGS, culminating in ventral prostate agenesis.

MATERIALS AND METHODS

Mice and dosing regimen. Mice were housed in polysulfone cages containing corn cob bedding and maintained on 12-h light/dark cycles at 21 ± 1°C and 20–50% relative humidity. Feed (Harlan Teklad Rodent Diet 8604, Harlan Laboratories Inc., Madison, WI) and water were available *ad libitum*. All procedures were approved by the University of Wisconsin Animal Care and Use Committee and conducted in accordance with the NIH Guide for Care and Use of Laboratory Animals. C57BL/6J mice were purchased from Jackson Laboratory (Bar Harbor, ME) and used for all ISH and IHC experiments. To obtain timed-pregnant dams, females were paired overnight with males. The next morning was considered E0.5. On E15.5, mouse fetuses were exposed *in utero* to corn oil vehicle alone (5 ml/kg dam, po) or corn oil containing TCDD (5 µg/kg dam, po, 98% purity, Cambridge Isotopes Laboratories, Andover, MA). The 5 µg/kg dose of TCDD is the highest dose that can be given to pregnant (E13.5–E15.5) C57BL/6J female mice that won't affect embryo viability, but still completely block ventral prostatic bud formation (Lin et al., 2002). Dams were euthanized by CO₂ asphyxiation at E16.0, E16.5, or E17.5.

In situ hybridization. UGSs were fixed overnight in 4% paraformaldehyde (PFA), dehydrated via graded incubations into 100% MeOH, and stored at –20°C until needed. On the day of sectioning, UGSs were rehydrated into PBS and cut with a vibrating microtome into 50 µm (sagittal) or 40 µm (transverse) sections. Riboprobe hybridization and staining procedures are described elsewhere (Abler et al., 2011; www.gudmap.org). Riboprobes were synthesized by PCR using primer sequences described previously (Mehta et al., 2011) that span sequences unique to each gene. The length of time required to stain sections after riboprobe hybridization varied from gene to gene depending on the relative abundance of RNA. Genes for which no RNA was detected were stained for up to 10 days before the procedure was stopped. Staining patterns in the UGS—which represent *in vivo* RNA transcription—were described for each riboprobe based on the analysis of sections from at least three litter-independent male embryos per treatment group. Descriptions of RNA transcription patterns were based on the anatomical ontology of the Edinburgh Mouse Atlas Project and modifications detailed by the GenitoUrinary Development Molecular Anatomy Project (GUDMAP, www.gudmap.org). Sections from vehicle- and TCDD-exposed UGSs were processed as a single unit so that RNA abundance and pattern could be compared between and within treatment groups. To ensure UGSs were processed in a manner that preserved high-quality RNA in all samples, we used a uroplakin 1b (*Upk1b*) riboprobe as a positive control and confirmed that *Upk1b* transcript was present in the expected abundance and pattern in at least one section from all vehicle- and TCDD-exposed UGSs used in this study.

Immunohistochemistry. UGS tissues were fixed overnight in 4% PFA, dehydrated into 100% ethanol, embedded in paraffin, and cut into 5 μ m sagittal sections. Before staining, sections were rehydrated, treated with 3% hydrogen peroxide for 10 min, boiled in 10 mM sodium citrate for 20 min, and allowed to cool to room temperature to unmask epitopes. Sections were blocked for 2 h with blocking solution – 5% goat serum (Sigma-Aldrich, G9023) and 1% bovine serum albumin (EMD Millipore, 2910) in phosphate buffered saline containing 0.05% Tween-20 (PBST; Sigma-Aldrich, P3563). Primary antibodies against NP-CTNNB1 (Cell Signaling, 8814) or LEF1 (Cell Signaling, 2230) were diluted 1:2000 and 1:250, respectively, in blocking solution, applied to the section, and incubated overnight at 4°C. Sections were washed with PBST and subsequently incubated for 1 h with biotinylated goat anti-rabbit IgG secondary antibody (Vector Labs, BA-1000) diluted 1:500 in blocking solution. Sections were washed with PBST and incubated for 30 min with peroxidase-conjugated streptavidin (Vector Labs, PK-6100). After washing with PBST, staining was achieved by incubating sections with 3,3'-diaminobenzidine (DAB) solution (Life Technologies, 002020) for 2–5 min at room temperature. Sections were counterstained with hematoxylin to label nuclei.

IHC quantification and statistics. Immunohistochemical staining for LEF1 is nuclear and clearly present or absent within a cell. Within the UGS, epithelial LEF1 expression roughly defines the regions (anterior, dorsal, lateral, ventral) from which prostatic buds will emerge, and is restricted to the first 1–2 cell layers proximal to the mesenchyme. As such, at E16.5, LEF1 expression does not extend into the epithelium of the bladder or urethra so no artificial or arbitrary intraepithelial boundaries were created. All LEF1-positive cells in the ventral epithelium of the UGS were counted. One LEF1-stained section from each of the 10 vehicle-exposed and six TCDD-exposed UGSs was counted. Each UGS was from a different litter.

The Wilcoxon Rank Sum test was used to determine if there was a significant difference in the number of LEF1-positive epithelial cells in the ventral UGS between vehicle-exposed and TCDD-exposed UGSs. A *p*-value of ≤ 0.05 was considered significant.

RESULTS

TCDD Alters Abundance and In Situ Localization of Wnt10a and Wnt16 RNAs in the UGS

The Wnt family of glycoproteins plays a central role in directing development, and recent studies have demonstrated that exposure to TCDD can alter Wnt signaling in a variety of tissues and cell types (Hrubá et al. 2011; Mathew et al., 2008; Procházková et al., 2011). We dosed pregnant C57BL/6J female mice with vehicle or TCDD (5 μ g/kg) at E15.5 and harvested UGSs from male embryos at E16.5, just prior to ventral prostatic budding initiation. ISH was used as an RNA detection method to evaluate both relative abundance and *in situ* localization. Of the 19 mouse Wnt genes, no staining was observed for five—Wnt1, 3, 8a, 8b, and 10b—indicating that either there was no transcript present, or transcript abundance was below detectable levels (Table 1, Supplementary table 1, and Supplementary figs. 1 and 2). Staining for an additional two genes—Wnt7a and 9b—was found only in the Mullerian ducts and Wolffian structures, respectively (Table 1, Supplementary table 1, and Supplementary fig. 2). Ten genes—Wnt2a, 2b, 3a, 4, 5a, 5b, 6, 7b, 9a, and 11—had detectable levels of staining in control UGSs which was unchanged by exposure to TCDD (Table 1, Supplementary table 1, and Supplemen-

tary figs. 1 and 2). Lastly, staining for two genes—Wnt10a and Wnt16—was altered in UGSs exposed to TCDD when compared with controls (Table 1). In control UGSs, strong Wnt10a staining was detected in the basal epithelium of the urethra, but in adjacent basal epithelium of the ventral UGS, staining intensity was markedly weaker to non-existent (Fig. 1A). By comparison, strong Wnt10a staining was detected in the basal epithelium of the urethra and continued all the way through the ventral UGS to the base of the bladder in TCDD-exposed UGSs (Fig. 1B). In control UGSs, Wnt16 staining was only detected in the mesenchyme immediately adjacent to the epithelium (lamina propria) in the urethra (Fig. 1C). In TCDD-exposed UGSs, Wnt16 staining covered a larger region. Like control UGSs, staining was detected in urethral mesenchyme, but also extended cranially into the mesenchyme of the ventral UGS, toward the bladder (Fig. 1D).

TCDD Alters RNA Abundance and In Situ Localization of Several Secreted and Transmembrane Modulators of Wnt Signaling

In addition to the Wnts, we used ISH to assess RNA abundance and localization for 27 genes known to play a role in Wnt signaling activation or modulation (Table 2, Supplementary table 2, and Supplementary figs. 3–5). Eleven of these genes encode proteins secreted into the extracellular space, 11 encode transmembrane proteins, and five encode intracellular proteins. At E16.5, there were two genes for which there was no detectable transcript in both vehicle- and TCDD-exposed UGSs, and one gene with staining restricted to the Wolffian structures only. Of the remaining 24 genes, three had detectably altered RNA abundance and *in situ* localization after exposure to TCDD: *Rspo2* (secreted protein), *Wif1* (secreted protein), and *Ror2* (transmembrane protein) (Table 2). Descriptions of *Rspo2* ISH results follow; results for *Wif1* and *Ror2* are described later.

At E16.5, in transverse sections of vehicle-exposed control UGSs, staining for *Rspo2* transcript was detected bilaterally in the ventral mesenchymal pads, and also as a complete ring running through the mesenchyme of the anterior and ventral budding regions (Supplementary fig. 6A). In sagittal sections, staining for *Rspo2* appears in the ventral mesenchymal pad with less intense staining also detectable in the anterior mesenchyme (Fig. 2A). By comparison, staining was less intense in both sagittal and transverse sections from age-matched, TCDD-exposed UGSs, indicating reduced *Rspo2* transcript abundance (Fig. 2B and Supplementary fig. 6B).

TCDD Reduces Accumulation of Non-Phosphorylated CTNNB1 (NP-CTNNB1) in Basal Epithelium of the Ventral UGS

Phosphorylation of CTNNB1 targets the protein for degradation, thus, preventing phosphorylation of CTNNB1 is required to activate CTNNB1 signaling. NP-CTNNB1 is stabilized, accumulates intracellularly, and translocates to the nucleus where it activates transcription of target genes. We dosed pregnant C57BL/6J dams with vehicle or TCDD (5 μ g/kg) at E15.5, harvested UGSs from male embryos at E16.0, E16.5, and E17.5, and assessed expression of NP-CTNNB1 by IHC. At E16.0 in control UGSs, NP-CTNNB1 staining was restricted to the cell membrane throughout the epithelium (Fig. 3A). However, around E16.5 we detected an overall increase in NP-CTNNB1 staining intensity in basal epithelial cells of the ventral UGS because, in addition to cell membranes, NP-CTNNB1 was also detected in the cytoplasm and nucleus of basal epithelial cells (Fig. 3B). By comparison, intermediate epithelial cells at E16.5 show no cytoplasmic accumulation or nuclear localization of NP-CTNNB1 (Fig. 3B). Thus, phosphorylation of CTNNB1 subsides around E16.5 in ventral basal epithelial cells in control UGSs and NP-CTNNB1 begins to accumulate

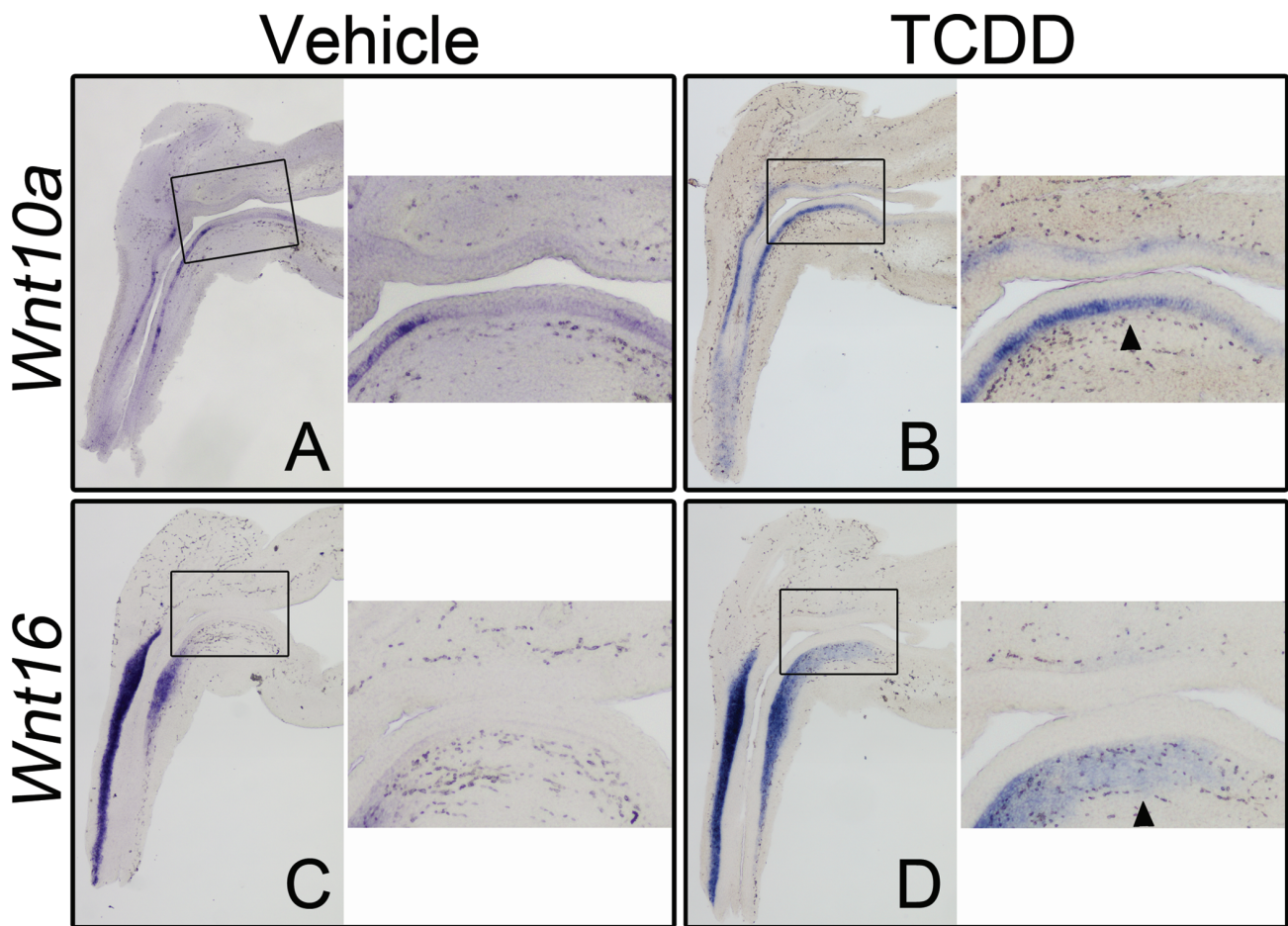


FIG. 1. TCDD increases *Wnt10a* and *Wnt16* transcript abundance in the ventral UGS. C57BL/6j mouse embryos were exposed *in utero* to vehicle or TCDD (5 $\mu\text{g}/\text{kg}$ dam, po) at E15.5 and UGSs were harvested at E16.5. UGSs were sectioned along the sagittal plane and are shown with the urethra on the left pointing down and the bladder on the right. Images are representative of at least eight litter-independent UGSs per treatment group. Within each panel, the boxed area in the left image is enlarged on the right. The purple stain marks transcript localization as assessed by ISH. *Wnt10a* transcription was restricted to the epithelium (A, B) whereas *Wnt16* transcription was restricted to the mesenchyme (C, D). Staining for *Wnt10a* and *Wnt16* in the ventral region of UGSs from vehicle control embryos is minimal to absent. However, staining for both *Wnt10a* and *Wnt16* is detectable in the ventral UGS after exposure to TCDD (arrowheads).

and translocate into the nucleus prior to initiation of ventral prostatic budding. By E17.5, prostatic buds are present in all budding regions of control UGSs. In the ventral basal epithelium, overall NP-CTNNB1 staining appears to be reduced compared with E16.5, with significant cytoplasmic accumulation and nuclear localization of NP-CTNNB1 most often observed in cells at the tips of prostatic buds (Fig. 3C).

At E16.0 in UGSs from TCDD-exposed embryos, NP-CTNNB1 staining was restricted to the cell membrane throughout the epithelium, and was not detectably different from controls (Fig. 3D). However, at E16.5 overall staining intensity of NP-CTNNB1 in TCDD-exposed UGSs failed to increase as it did in the controls and NP-CTNNB1 nuclear localization was largely absent (Fig. 3E). Thus, *in utero* TCDD exposure likely causes CTNNB1 phosphorylation to persist inappropriately, preventing CTNNB1 accumulation in basal epithelial cells of the ventral UGS. At E17.5, no ventral buds were present, and there was little to no cytoplasmic accumulation or nuclear localization of NP-CTNNB1 indicating sustained CTNNB1 phosphorylation and degradation after exposure to TCDD.

TCDD Reduces LEF1 Expression in Basal Epithelium of the Ventral UGS
Active CTNNB1 signaling is capable of inducing LEF1 expression in multiple tissues including the UGS (Francis et al., 2013; Mehta et al., 2013). We assessed LEF1 expression in vehicle- and TCDD-exposed UGSs by IHC. In control UGSs, LEF1 expression was detected in the lamina propria of the urethra, UGS, and bladder at E14.5, the earliest time tested, and persisted through E18.5, the latest time tested (Fig. 4 and Schneider, unpublished data). Around E16.5, LEF1 expression was induced in basal epithelial cells of the ventral UGS prior to bud initiation, and continued through the initiation and elongation stages of bud development (Fig. 4A). Thus, induction of epithelial LEF1 expression corresponded with the cytoplasmic accumulation and nuclear localization of NP-CTNNB1 discussed above, and, importantly, we never detected epithelial LEF1 expression without nuclear NP-CTNNB1.

In TCDD-exposed UGSs, mesenchymal LEF1 expression matched that observed in control UGSs, but epithelial LEF1 expression at E16.5 was greatly reduced compared with vehicle controls (Fig. 4B). The number of basal epithelial cells expressing LEF1 in the ventral UGS was reduced from 37 ± 8 cells (mean \pm SE) in control UGSs to 1 ± 1 cell in TCDD-exposed UGSs; $p < 0.0002$ (Fig. 4C). The ventral region of E17.5 TCDD-exposed UGSs

TABLE 1. Effect of *In Utero* TCDD Exposure on Abundance and Localization of RNA from Wnt Genes in Mouse UGS at E16.5^a

RNA transcript	Epithelium		Mesenchyme			
	Basal ^b	Intermediate ^c	Ventral lamina propria ^d	Ventral	Dorsolateral	Anterior
Wnt Ligands						
<i>Wnt1</i>						
<i>Wnt2a</i>				↔		↔
<i>Wnt2b</i>	↔	↔		↔	↔	↔
<i>Wnt3</i>						
<i>Wnt3a</i>	↔	↔	↔	↔	↔	↔
<i>Wnt4</i>		↔				
<i>Wnt5a</i>			↔	↔	↔	↔
<i>Wnt5b</i>				↔	↔	↔
<i>Wnt6</i>	↔					
<i>Wnt7a</i>						
<i>Wnt7b</i>		↔				
<i>Wnt8a</i>						
<i>Wnt8b</i>						
<i>Wnt9a</i>			↔	↔	↔	↔
<i>Wnt9b</i>						
<i>Wnt10a</i>	↑					
<i>Wnt10b</i>						
<i>Wnt11</i>			↔	↔	↔	↔
<i>Wnt16</i>			↑			

^aAt least three litter-independent UGSs per treatment group were used to determine RNA abundance and localization for each gene. Corn oil (vehicle) or TCDD (5 µg/kg, po) was administered to pregnant dams on E15.5. A horizontal arrow denotes that RNA was detected in the indicated tissue compartment and that there was no detectable difference in RNA abundance or localization between vehicle- and TCDD-exposed UGSs at E16.5. Upward-pointing arrows indicate that TCDD increased transcript abundance compared with vehicle-exposed control UGSs. No arrow indicates that transcript was not detected.

^bBasal epithelium = epithelial cells bordering mesenchyme.

^cIntermediate epithelium = epithelial cells that do not border mesenchyme or lumen.

^dVentral lamina propria = mesenchyme immediately adjacent to the epithelium in the ventral UGS.

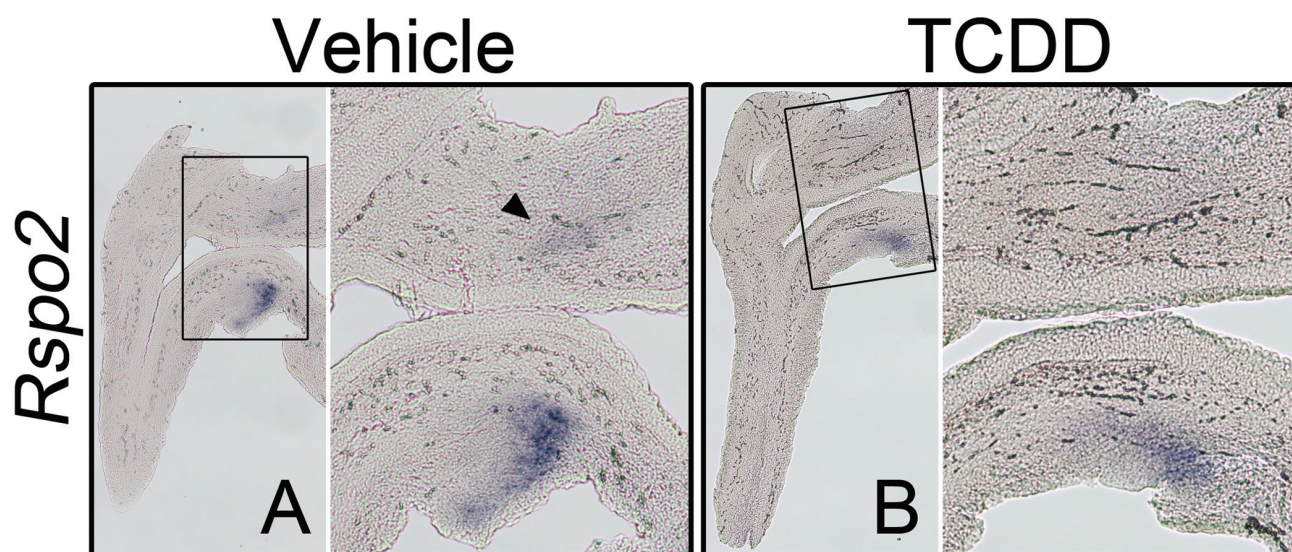


FIG. 2. TCDD reduces transcript abundance of *Rspo2* in UGS mesenchyme. C57BL/6J mouse embryos were exposed *in utero* to vehicle or TCDD (5 µg/kg dam, po) at E15.5 and UGSs were harvested at E16.5. UGSs were sectioned along the sagittal plane and are shown with the urethra on the left pointing down and the bladder on the right. Images are representative of at six litter-independent UGSs per treatment group. Within each panel, the boxed area in the left image is enlarged on the right. The purple stain marks transcript localization as assessed by ISH. *Rspo2* transcription was restricted to the mesenchyme (A, B). The arrowhead in (A) points to faint staining in the anterior mesenchyme of the UGS. Exposure to TCDD reduces abundance of *Rspo2* RNA.

TABLE 2. Effect of *In Utero* TCDD Exposure on Abundance and Localization of RNA from Wnt Signaling Modulators in Mouse UGS at E16.5^a

RNA Transcript	Epithelium		Mesenchyme			
	Basal ^b	Intermediate ^c	Ventral Lamina Propria ^d	Ventral	Dorsolateral	Anterior
Extracellular^e						
<i>Dkk1</i>	↔	↔	↔	↔	↔	↔
<i>Dkk2</i>	↔	↔	↔	↔	↔	↔
<i>Frzb (Sfrp3)</i>			↔	↔	↔	
<i>Rspo1</i>				↔		↔
<i>Rspo2</i>				↔		↔
<i>Rspo3</i>				↔	↔	↔
<i>Rspo4</i>						
<i>Sfrp1</i>						
<i>Sfrp2</i>			↔	↔	↔	↔
<i>Sfrp4</i>				↔	↔	↔
<i>Wif1</i>	↓		↓	↓	↓	↓
Transmembrane^e						
<i>Fzd6</i>	↔	↔			↔	
<i>Fzd7</i>		↔	↔	↔	↔	↔
<i>Fzd8</i>						
<i>Fzd10</i>	↔	↔	↔			
<i>Kremen1</i>		↔				
<i>Lgr4</i>	↔	↔				
<i>Lgr5</i>	↔	↔				
<i>Lrp5</i>	↔	↔				
<i>Lrp6</i>	↔	↔		↔	↔	
<i>Ror1</i>				↔	↔	↔
<i>Ror2</i>		↓				
Intracellular^e						
<i>Axin2</i>	↔		↔		↔	↔
<i>Hnf1b (Tcf2)</i>	↔	↔	↔	↔	↔	↔
<i>Tcf1</i>	↔	↔	↔	↔	↔	↔
<i>Tcf711</i>	↔		↔	↔	↔	↔
<i>Tcf712</i>	↔			↔	↔	↔

^aAt least three litter-independent UGSs per treatment group were used to determine RNA abundance and localization for each gene. Corn oil (vehicle) or TCDD (5 µg/kg, po) was administered to pregnant dams on E15.5. A horizontal arrow denotes that RNA was detected in the indicated tissue compartment and that there was no detectable difference in RNA abundance or localization between vehicle- and TCDD-exposed UGSs at E16.5. Downward-pointing arrows indicate that TCDD decreased transcript abundance compared with vehicle-exposed control UGSs. No arrow indicates that transcript was not detected.

^bBasal epithelium = epithelial cells bordering mesenchyme.

^cIntermediate epithelium = epithelial cells that do not border mesenchyme or lumen.

^dVentral lamina propria = mesenchyme immediately adjacent to the epithelium in the ventral UGS.

^eBecause the reported functions of Wnt signaling modulators can vary from system to system, genes were sorted by the subcellular localization of their proteins rather than sorted by function.

resembled that of E16.5 TCDD-exposed UGSs – no buds and little to no LEF1 expression in basal epithelial cells, which demonstrates persistent downregulation of CTNNB1 signaling by TCDD (Fig. 4D). In sharp contrast to the ventral region, LEF1 expression was detected throughout the anterior basal epithelium, including in developing buds (Fig. 4D). LEF1-stained, TCDD-exposed, E17.5 UGSs clearly illustrate that TCDD inhibits CTNNB1 signaling in a region-specific manner, while also providing additional evidence that CTNNB1-signaling is required in the basal epithelium to induce budding.

TCDD Reduces *Wif1* Transcript Abundance in Basal Epithelium of the Ventral UGS

WIF1 is a secreted antagonist of Wnt/CTNNB1 signaling, but has also been identified as a CTNNB1 signaling target gene in several cell lines and tissues, including UGS epithelium (Ha et al., 2012; Mehta et al., 2013). We assessed *Wif1* transcript localization and abundance by ISH in vehicle- and TCDD-exposed UGSs.

At E16.5, strong mesenchymal staining was detected in both control and TCDD-exposed UGSs; however, *Wif1* transcription in the mesenchyme is not regulated by CTNNB1 signaling (Keil et al., 2012). In control UGSs, *Wif1* transcript was also detected in basal epithelium of both the anterior and ventral UGS, as well as the epithelium of developing buds (Fig. 5A). In age-matched, TCDD-exposed UGSs, *Wif1* transcript abundance was decreased in basal epithelium of the ventral UGS, further demonstrating reduced CTNNB1 signaling after TCDD exposure (Fig. 5B).

TCDD Reduces RNA Abundance for *Ror2*, a Putative CTNNB1 Signaling Target Gene, in Ventral UGS Epithelium

ROR2 is a single-pass transmembrane receptor that can potentiate multiple Wnt signaling cascades including the Wnt/CTNNB1 signaling cascade (Li et al., 2008; Nishita et al., 2010). At E16.5, in control UGSs, *Ror2* is transcribed in the epithelium of all initiated and elongating buds (anterior and dorsolateral regions) as well as in the UGS epithelium of anterior, dorsolateral, and ven-

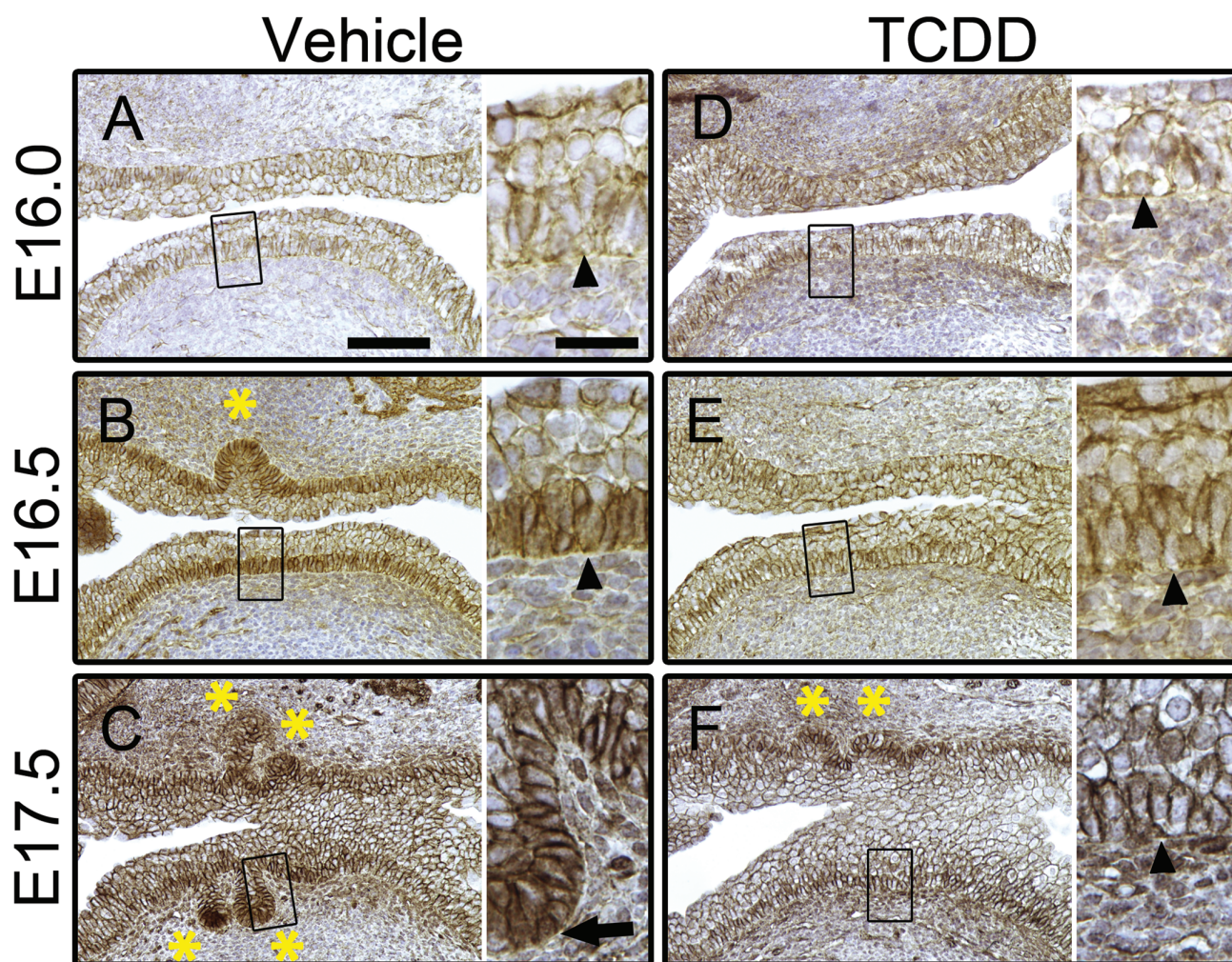


FIG. 3. TCDD prevents accumulation and nuclear localization of NP-CTNNB1. C57BL/6j mouse embryos were exposed *in utero* to vehicle or TCDD (5 $\mu\text{g}/\text{kg}$ dam, po) at E15.5 and UGSs were harvested at E16.0, E16.5, or E17.5. UGSs were sectioned along the sagittal plane and the anterior and ventral budding regions are shown (bladder is to the right in each image). Images are representative of at least three litter-independent UGSs per treatment group. In each panel, the image on the left is shown at 100X (scale bar represents 100 μm) and the boxed region is shown on the right at 200X (scale bar represents 25 μm). IHC staining using DAB as the chromogen (brown) shows subcellular localization of NP-CTNNB1; nuclei are counterstained with hematoxylin (blue). Arrowheads point to ventral basal epithelial cells; asterisks mark prostatic buds. In E16.0 vehicle-exposed UGSs, NP-CTNNB1 is restricted to cell membranes (A). By E16.5 in vehicle-exposed UGSs cytoplasmic accumulation and nuclear localization of NP-CTNNB1 is detectable in the ventral basal epithelial cells—note that the nuclei of intermediate epithelial cells are devoid of CTNNB1 staining (B). At E17.5, in vehicle-exposed UGSs, anterior and ventral prostatic buds are visible, with NP-CTNNB1 nuclear localization primarily seen in bud tips (arrow in C). *In utero* exposure to TCDD has no effect on subcellular localization of NP-CTNNB1 at E16.0 (D). However, at E16.5 (E) and E17.5 (F) TCDD-exposed UGSs show no NP-CTNNB1 accumulation in the cytoplasm, no NP-CTNNB1 nuclear localization, and no ventral buds.

tral budding regions (Fig. 5C and Schneider *et al.*, unpublished data). Notably, the basal cell layer is generally devoid of staining whereas the intermediate cell layer shows staining (Table 2). In age-matched UGSs exposed to TCDD, little to no *Ror2* transcript was observed (Fig. 5D).

Like *Lef1* and *Wif1*, *Ror2* might also be a CTNNB1 signaling target gene. UGSs genetically engineered to overexpress CTNNB1 in the epithelium develop clusters of cells that express high levels of CTNNB1 (Supplementary fig. 7A and Mehta *et al.*, 2013). When these UGSs are probed by ISH for known target genes *Lef1* and *Wif1*, strong staining is observed in the CTNNB1-positive cell clusters (Mehta *et al.*, 2013). Similarly, these CTNNB1-positive cell clusters also stain positively for *Ror2* suggesting that *Ror2* is a CTNNB1 signaling target gene in UGS epithelium (Supplementary fig. 7B).

DISCUSSION

TCDD is a potent teratogen in the mouse, and one of the consequences of *in utero* exposure is complete inhibition of ventral prostatic budding, culminating in ventral prostate agenesis (Lin *et al.*, 2003; Vezina *et al.*, 2008). We previously established that budding inhibition occurs when TCDD activates AHR in the UGS mesenchyme (Ko *et al.*, 2004a), yet the subsequent alterations to the mesenchymally derived paracrine signaling that induces prostatic budding are not fully understood. Wnt signaling is required for prostate development, and given that most Wnts are expressed in the UGS (Mehta *et al.*, 2011; Zhang *et al.*, 2006), it is likely that multiple Wnt signaling cascades are active during the budding process. Importantly, a well-regulated balance must be attained as both downregulation and upregulation of Wnt signaling can impair normal prostatic bud formation (Allgeier *et al.*, 2008; Branam *et al.*, 2013; Francis *et al.*, 2013; Huang *et al.*, 2009;

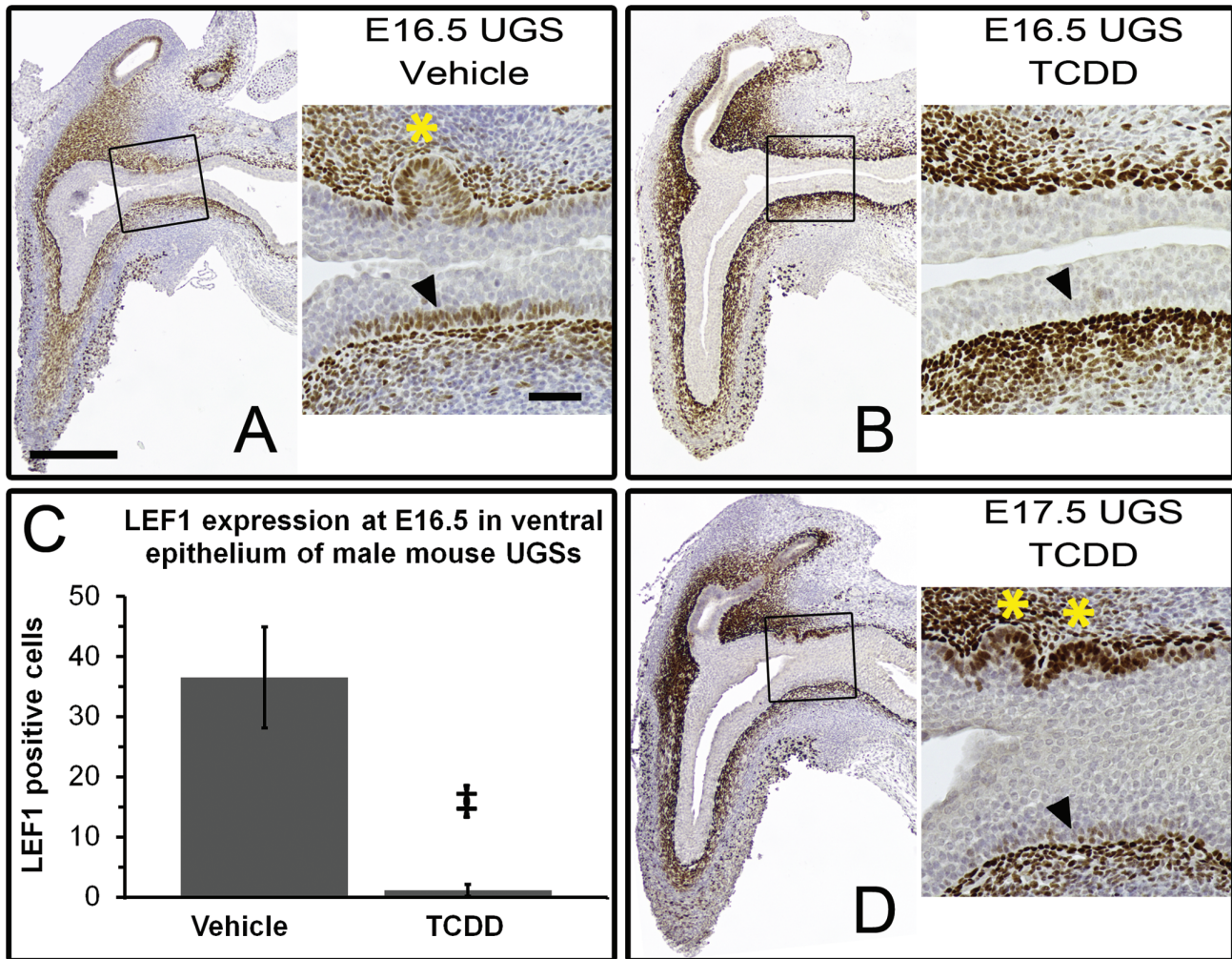


FIG. 4. TCDD reduces LEF1 expression in basal epithelium of the ventral UGS. C57BL/6J mouse embryos were exposed *in utero* to vehicle or TCDD (5 $\mu\text{g}/\text{kg}$ dam, po) at E15.5 and UGSs were harvested at E16.5 or E17.5. UGSs were sectioned along the sagittal plane and are shown with the urethra on the left pointing down and the bladder on the right. Images are representative of at least six litter-independent UGSs per treatment group. In panels (A), (B), and (D), images on the left are magnified 40X (scale bar represents 300 μm), with the boxed areas shown to the right at 100X (scale bar represents 100 μm). IHC staining using DAB as the chromogen (brown) marks LEF1 positive cells; nuclei are counterstained with hematoxylin (blue). Arrowheads point to ventral basal epithelial cells; asterisks mark prostatic buds. Around E16.5 in vehicle-exposed UGSs, LEF1 expression is initiated in the ventral epithelium (A). TCDD prevents LEF1 expression in the ventral epithelium at E16.5 (B). This difference was quantified by counting and averaging all LEF1-positive cells in the ventral epithelium in a single sagittal section from 10 vehicle-exposed and six TCDD-exposed E16.5 UGSs (C). The double dagger symbol (\ddagger) indicates a statistically significant difference ($p < 0.0002$). At E17.5 there is still little to no LEF1 expression in the ventral epithelium, however LEF1 staining is seen in the anterior epithelium (D). Correspondingly, prostatic budding has initiated in the anterior UGS but not the ventral UGS.

Mehta et al., 2013; Simons et al., 2012). Recently, we and others have demonstrated that exposure to TCDD can downregulate the Wnt/CTNNB1 signaling cascade *in vitro* (Branam et al., 2013; Hrubá et al. 2011; Procházková et al., 2011). In this study, we assessed Wnt signaling *in vivo*, using UGSs from both vehicle- and TCDD-exposed male mouse embryos. We found that (1) Wnt signaling is active in the UGS at E16.5 as we detected RNA from a majority of the 46 genes surveyed; (2) in control UGSs, CTNNB1 signaling is activated in the ventral epithelium around E16.5, just before ventral budding initiation; (3) *in utero* TCDD exposure altered RNA abundance for five of the 46 genes surveyed by ISH; and (4) TCDD blocked activation of CTNNB1 signaling.

TCDD Prevents Accumulation of NP-CTNNB1 and Activation of CTNNB1 Signaling

Around E16.5, just prior to ventral bud initiation, NP-CTNNB1 begins to accumulate and translocate into the nucleus of basal

epithelial cells of the ventral UGS. Coincident with nuclear localization of NP-CTNNB1 is an upregulation of LEF1 expression. *Lef1* has previously been identified as a CTNNB1 target gene in the UGS epithelium (Branam et al., 2013; Francis et al., 2013; Mehta et al., 2013), and, correspondingly, we never observed epithelial LEF1 expression without CTNNB1 nuclear localization. Though these data do not elucidate the activating stimulus that prevents CTNNB1 phosphorylation, they do demonstrate that there is active signaling through CTNNB1 in the basal epithelium of the ventral UGS prior to budding.

In utero exposure to TCDD at E15.5 caused a pronounced decrease in NP-CTNNB1 accumulation and a concomitant decrease in expression and transcript abundance, respectively, of CTNNB1 target genes *Lef1* and *Wif1* in the ventral epithelium of UGSs at E16.5. Furthermore, *Ror2*, which is a putative CTNNB1 target gene in the UGS epithelium, also demonstrated decreased transcript abundance after exposure to TCDD. We and others

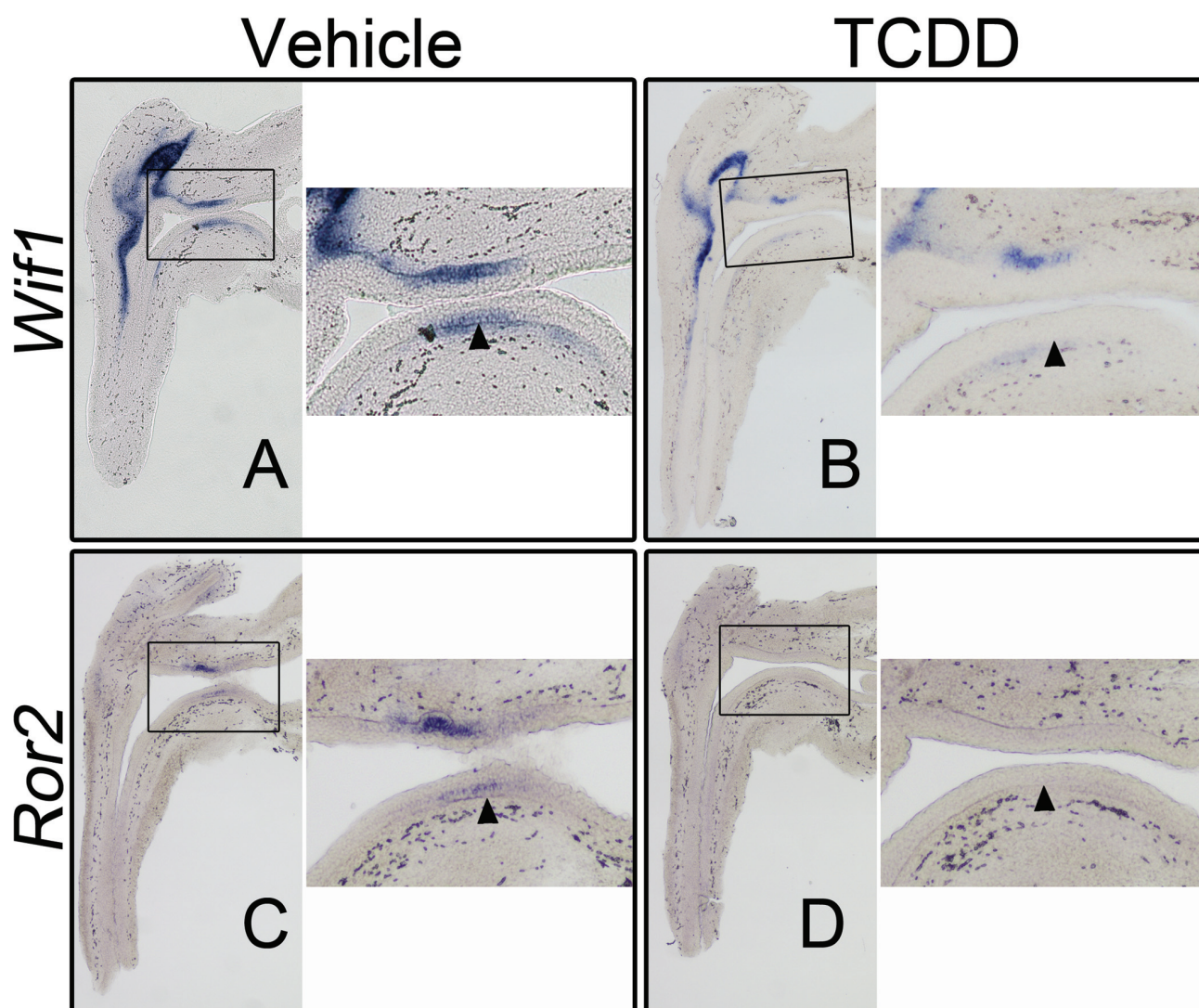


FIG. 5. TCDD reduces transcript abundance of known, *Wif1*, and putative, *Ror2*, CTNNB1 signaling target genes in ventral UGS epithelium. C57BL/6J mouse embryos were exposed *in utero* to vehicle or TCDD (5 $\mu\text{g}/\text{kg}$ dam, po) at E15.5 and UGSs were harvested at E16.5. UGSs were sectioned along the sagittal plane and are shown with the urethra on the left pointing down and the bladder on the right. Images are representative of three (*Ror2*) and six (*Wif1*) litter-independent UGSs per treatment group. Within each panel, the boxed area in the left image is enlarged on the right. The purple stain marks transcript localization as assessed by ISH and arrowheads point to ventral basal epithelial cells. In vehicle-exposed UGSs, *Wif1* transcript is detectable in the ventral epithelium in the same region where nuclear CTNNB1 and LEF1 expression is observed (A). *Wif1* RNA abundance is decreased in the ventral epithelium in TCDD-exposed UGSs (B). Similar to *Wif1*, *Ror2* transcript is observed in the ventral epithelium of vehicle-exposed UGSs (C). Exposure to TCDD reduces abundance of *Ror2* RNA (D).

have demonstrated that knockout of *Ctnnb1* in the UGS prevents prostatic budding; therefore, this downregulation of CTNNB1 signaling by *in utero* TCDD exposure could explain why ventral buds do not develop (Francis *et al.*, 2013; Lin *et al.*, 2012; Mehta *et al.*, 2013; Simons *et al.*, 2012). We attempted to restore ventral budding to the UGSs of TCDD-exposed embryos, by overexpressing a stabilized form of CTNNB1 in the UGS epithelium, but we found that, similar to other reports, excess CTNNB1 signaling is also capable of inhibiting prostatic budding (Francis *et al.*, 2013; Lin *et al.*, 2012; Mehta *et al.*, 2013).

TCDD Alters RNA Abundance and In Situ Localization of Several Wnt Signaling Modulators

ISH staining allowed us to detect changes in both relative abundance and localization of RNA after exposure to TCDD. TCDD altered RNA abundance and localization for five genes, generally increasing staining for *Wnt10a* and *Wnt16*, while simultaneously

decreasing staining for *Ror2*, *Rspo2*, and *Wif1*. However, there are several caveats to consider when interpreting these ISH findings: (1) we assessed RNA abundance and localization at only one developmental time point (E16.5); (2) initiation of transcription for *Ror2*, *Rspo2*, and *Wif1* in the ventral UGS appears to be around E16.5; and (3) we previously reported that *in utero* exposure to TCDD delays prostatic budding in the anterior and dorsolateral regions of the UGS by about 24 h (Lin *et al.*, 2003). Therefore, we cannot say if the decreases in RNA abundance are sustained indefinitely, or are due to a TCDD-induced developmental delay. Nonetheless, delayed Wnt signaling could be sufficient to cause ventral prostate agenesis because Simons *et al.* (2012) have proposed that CTNNB1 signaling is required between E14.5 and E16.5 for normal prostatic differentiation to occur. TCDD could delay activation of CTNNB1 signaling until this developmental window has passed.

Significance of *Wnt16* Transcription in the Ventral UGS after Exposure to TCDD

TCDD-induced activation of AHR in the UGS mesenchyme is the initial stimulus that causes prostatic budding failure in the ventral UGS epithelium (Ko et al., 2004a). We show here that TCDD subsequently blocks CTNNB1 signaling in the ventral basal epithelium. We have also presented data that make *Wnt16* a putative link between the mesenchymal site of action for TCDD and the epithelial outcome of downregulated CTNNB1 signaling. At E16.5 in control UGSs, *Wnt16* transcript is detected only in the mesenchyme around the urethra, but in age-matched TCDD-exposed UGSs, transcript is also detected in the ventral UGS mesenchyme. This finding suggests TCDD induces ectopic WNT16 expression in the ventral mesenchyme, thereby generating a known paracrine signal (Sun et al., 2012) that could alter Wnt signaling in the ventral epithelium. Multiple studies have shown that WNT16 either does (Jiang et al., 2014; Mazieres et al., 2005; Sun et al., 2012) or does not (Binet et al., 2009; Clements et al., 2011; Lu et al., 2004; Nygren et al., 2009; Teh et al., 2007) activate CTNNB1 signaling, with the end result likely dependent upon which other regulators of Wnt signaling are also present in the tissue. There are at least two plausible mechanisms by which WNT16 could alter Wnt signaling so as to inhibit CTNNB1 signaling: by out-competing ligands that activate CTNNB1 signaling for cell surface receptors or by activating a signaling cascade that prevents CTNNB1 stabilization and accumulation. Thus, WNT16 is an attractive candidate as a protein that has a direct role in inhibiting ventral budding because TCDD induces its expression in the ventral UGS mesenchyme, and WNT16 could be capable of blocking activation of CTNNB1 signaling.

Significance of Reduced *Rspo2* Transcript Abundance after Exposure to TCDD

At E16.5, *Rspo2* is transcribed in a ring around the epithelium of the anterior and ventral budding regions. In sagittal sections, this appears as staining in the anterior mesenchyme and ventral mesenchymal pads, which are subcompartments of the UGS mesenchyme known to produce signaling factors essential for ventral prostate development (reviewed in Thomson, 2008). ISH data from E17.5 UGSs (Mehta et al., 2011) show that staining for *Rspo2* transcript is more intense and covers a moderately larger area, suggesting that *Rspo2* transcription starts not long before E16.5. Therefore, the reduced *Rspo2* transcript abundance observed at E16.5 in TCDD-exposed UGSs could be due to a delay in the onset of *Rspo2* transcription rather than a sustained transcriptional decrease. *In vitro* experiments showed reduced *Rspo2* transcript abundance in UGSs cultured with TCDD for two days, but no difference was observed in control versus TCDD-exposed UGSs after three or four days in culture, suggesting TCDD delays the onset of *Rspo2* transcription (Branam et al., 2013).

RSPO2 is a paracrine signaling protein that can activate CTNNB1 signaling (reviewed in Jin and Yoon, 2012). Given the robust *Rspo2* transcription observed in the ventral mesenchymal pads, it is likely that the ventral epithelium is the target tissue for RSPO2 protein. *In vitro*, RSPO2 promotes prostatic budding. UGSs cultured with exogenous RSPO2 developed significantly more buds compared with controls. Furthermore, although UGSs cultured with TCDD had reduced bud number and epithelial CTNNB1 signaling compared with control UGSs, culture with TCDD plus RSPO2 restored bud number to that of controls and increased epithelial CTNNB1 signaling (Branam et al., 2013). Other TCDD-induced developmental defects could also be linked to the downregulation of RSPO2 expression because *Rspo2* knockout mice develop with a cleft palate and hypomor-

phic lungs which are also teratogenic outcomes of *in utero* TCDD exposure (Couture et al., 1990; Kransler et al., 2009; Yamada et al., 2009). Thus, like *Wnt16*, *Rspo2* is another attractive candidate gene with a potential role in the impaired ventral prostatic budding phenotype. However, opposite of *Wnt16*, it is the TCDD-induced downregulation of RSPO2 in UGS mesenchyme that could directly result in decreased CTNNB1 signaling in the epithelium.

TCDD and Wnt Signaling

Wnt signaling encompasses a number of different signaling cascades and is capable of regulating diverse biological responses. How Wnt signaling affects a biological response seems to depend on the combination of Wnt ligands, receptors, coreceptors, agonists, and antagonists that are present. Therefore, TCDD-induced inhibition of ventral prostatic budding might not be due to the altered expression of any one gene in the Wnt signaling pathway, but rather, due to the multiple changes we have reported here that, cumulatively, alter the well-regulated balance of all Wnt signaling cascades.

SUPPLEMENTARY DATA

Supplementary data are available online at <http://toxsci.oxfordjournals.org/>.

FUNDING

National Institutes of Health (ES01332). Funding for open access charge: National Institute of Environmental Health Sciences.

ACKNOWLEDGMENT

We would like to thank Joan Palmer for her assistance with manuscript formatting.

REFERENCES

- Abbott, B. D., Lin, T. M., Rasmussen, N. T., Albrecht, R. M., Schmid, J. E. and Peterson, R. E. (2003). Lack of expression of EGF and TGF- α in the fetal mouse alters formation of prostatic epithelial buds and influences the response to TCDD. *Toxicol. Sci.* **76**, 427–436.
- Abler, L. L., Mehta, V., Keil, K. P., Joshi, P. S., Flucus, C. L., Hardin, H. A., Schmitz, C. T. and Vezina, C. M. (2011). A high throughput *in situ* hybridization method to characterize mRNA expression patterns in the fetal mouse lower urogenital tract. *J. Vis. Exp.* **54**, e2912.
- Allgeier, S. H., Lin, T. M., Vezina, C. M., Moore, R. W., Fritz, W. A., Chiu, S. Y., Zhang, C. and Peterson, R. E. (2008). WNT5A selectively inhibits mouse ventral prostate development. *Dev. Biol.* **324**, 10–17.
- Binet, R., Ythier, D., Robles, A. I., Collado, M., Larriue, D., Fonti, C., Brambilla, E., Brambilla, C., Serrano, M., Harris, C. C., et al. (2009). WNT16B is a new marker of cellular senescence that regulates p53 activity and the phosphoinositide 3-kinase/AKT pathway. *Cancer Res.* **69**, 9183–9191.
- Birnbaum, L. S. and Fenton, S. E. (2003). Cancer and developmental exposure to endocrine disruptors. *Environ. Health Perspect.* **111**, 389–394.
- Branam, A. M., Davis, N. M., Moore, R. W., Schneider, A. J., Vezina, C. M. and Peterson, R. E. (2013). TCDD inhibition of canonical Wnt signaling disrupts prostatic bud formation in mouse

- urogenital sinus. *Toxicol. Sci.* **133**, 42–53.
- Clements, W. K., Kim, A. D., Ong, K. G., Moore, J. C., Lawson, N. D. and Traver, D. (2011). A somitic Wnt16/Notch pathway specifies haematopoietic stem cells. *Nature* **474**, 220–225.
- Couture, L. A., Abbott, B. D. and Birnbaum, L. S. (1990). A critical review of the developmental toxicity and teratogenicity of 2,3,7,8-tetrachlorodibenzo-*p*-dioxin: recent advances toward understanding the mechanism. *Teratology* **42**, 619–627.
- Craig, Z. R., Wang, W. and Flaws, J. A. (2011). Endocrine-disrupting chemicals in ovarian function: effect on steroidogenesis, metabolism and nuclear receptor signaling. *Reproduction* **142**, 633–646.
- Cunha, G. R. (2008). Mesenchymal-epithelial interactions: Past, present, and future. *Differentiation* **76**, 578–586.
- Francis, J. C., Thomsen, M. K., Taketo, M. M. and Swain, A. (2013). β -catenin is required for prostate development and cooperates with Pten loss to drive invasive carcinoma. *PLoS Genet.* **9**, e1003180.
- Ha, A., Perez-Iratxeta, C., Liu, H., Mears, A. J. and Wallace, V. A. (2012). Identification of Wnt/beta-catenin modulated genes in the developing retina. *Mol. Vis.* **18**, 645–656.
- Hrubá, E., Vondráček, J., Líbalová, H., Topinka, J., Bryja, V., Souček, K. and Machala, M. (2011). Gene expression changes in human prostate carcinoma cells exposed to genotoxic and nongenotoxic aryl hydrocarbon receptor ligands. *Toxicol. Lett.* **206**, 178–188.
- Huang, L., Pu, Y., Hu, W. Y., Birch, L., Luccio-Camelo, D., Yamaguchi, T. and Prins, G. S. (2009). The role of Wnt5a in prostate gland development. *Dev. Biol.* **328**, 188–199.
- Jiang, Z., Von den Hoff, J. W., Torensma, R., Meng, L. and Bian, Z. (2014). Wnt16 is involved in intramembranous ossification and suppresses osteoblast differentiation through the Wnt/ β -catenin pathway. *J. Cell. Physiol.* **229**, 384–392.
- Jin, Y. R. and Yoon, J. K. (2012). The R-spondin family of proteins: Emerging regulators of WNT signaling. *Int. J. Biochem.* **44**, 2278–2287.
- Kawajiri, K., Kobayashi, Y., Ohtake, F., Ikuta, T., Matsushima, Y., Mimura, J., Pettersson, S., Pollenz, R. S., Sakaki, T., Hirokawa, T., et al. (2009). Aryl hydrocarbon receptor suppresses intestinal carcinogenesis in *Apc^{Min/+}* mice with natural ligands. *Proc. Natl. Acad. Sci. U.S.A.* **106**, 13481–13486.
- Keil, K. P., Mehta, V., Branam, A. M., Ablner, L. L., Buresh-Stiemke, R. A., Joshi, P. S., Schmitz, C. T., Marker, P. C. and Vezina, C. M. (2012). Wnt inhibitory factor 1 (*Wif1*) is regulated by androgens and enhances androgen-dependent prostate development. *Endocrinology* **153**, 6091–6103.
- Kerkvliet, N. I. (2009). AHR-mediated immunomodulation: The role of altered gene transcription. *Biochem. Pharmacol.* **77**, 746–760.
- Kharaishvili, G., Simkova, D., Makharoblidze, E., Trtkova, K., Kolar, Z. and Bouchal, J. (2011). Wnt signaling in prostate development and carcinogenesis. *Biomed. Pap. Med. Fac. Univ. Palacky Olomouc Czech Repub.* **155**, 11–18.
- King-Heiden, T. C., Mehta, V., Xiong, K. M., Lanham, K. A., Antkiewicz, D. S., Ganser, A., Heideman, W. and Peterson, R. E. (2012). Reproductive and developmental toxicity of dioxin in fish. *Mol. Cell. Endocrinol.* **354**, 121–138.
- Knerr, S. and Schrenk, D. (2006). Carcinogenicity of 2,3,7,8-tetrachlorodibenzo-*p*-dioxin in experimental models. *Mol. Nutr. Food Res.* **50**, 897–907.
- Ko, K., Moore, R. W. and Peterson, R. E. (2004a). Aryl hydrocarbon receptors in urogenital sinus mesenchyme mediate the inhibition of prostatic epithelial bud formation by 2,3,7,8-tetrachlorodibenzo-*p*-dioxin. *Toxicol. Appl. Pharmacol.* **196**, 149–155.
- Ko, K., Theobald, H. M., Moore, R. W. and Peterson, R. E. (2004b). Evidence that inhibited prostatic epithelial bud formation in 2,3,7,8-tetrachlorodibenzo-*p*-dioxin-exposed C57BL/6J fetal mice is not due to interruption of androgen signaling in the urogenital sinus. *Toxicol. Sci.* **79**, 360–369.
- Kransler, K. M., McGarrigle, B. P., Swartz, D. D. and Olson, J. R. (2009). Lung development in the Holtzman rat is adversely affected by gestational exposure to 2,3,7,8-tetrachlorodibenzo-*p*-dioxin. *Toxicol. Sci.* **107**, 498–511.
- Leng, L., Chen, X., Li, C.-P., Luo, X.-Y. and Tang, N.-J. (2014). 2,3,7,8-Tetrachlorodibenzo-*p*-dioxin exposure and prostate cancer: A meta-analysis of cohort studies. *Public Health* **128**, 207–213.
- Li, C., Chen, H., Hu, L., Xing, Y., Sasaki, T., Villosio, M. F., Li, J., Nishita, M., Minami, Y. and Minoo, P. (2008). Ror2 modulates the canonical Wnt signaling in lung epithelial cells through cooperation with Fzd2. *BMC Mol. Biol.* **9**, 11.
- Lin, T.-M., Bai, J. and Peterson, R.E. (2012). Early stabilization of β -catenin in urogenital sinus (UGS) epithelia disrupts mouse ventral prostate (VP) development. *Toxicol. Sci.* **126**(Suppl. 1), 2357 (Abstract).
- Lin, T.-M., Ko, K., Moore, R. W., Simanainen, U., Oberley, T. D. and Peterson, R.E. (2002). Effects of aryl hydrocarbon receptor null mutation and *in utero* and lactational 2,3,7,8-tetrachlorodibenzo-*p*-dioxin exposure on prostate and seminal vesicle development in C57BL/6 mice. *Toxicol. Sci.* **68**, 479–487.
- Lin, T.-M., Rasmussen, N. T., Moore, R. W., Albrecht, R. M. and Peterson, R. E. (2003). Region-specific inhibition of prostatic epithelial bud formation in the urogenital sinus of C57BL/6 mice exposed *in utero* to 2,3,7,8-tetrachlorodibenzo-*p*-dioxin. *Toxicol. Sci.* **76**, 171–181.
- Lu, D., Zhao, Y., Tawatao, R., Cottam, H. B., Sen, M., Leoni, L. M., Kipps, T. J., Corr, M. and Carson, D. A. (2004). Activation of the Wnt signaling pathway in chronic lymphocytic leukemia. *Proc. Natl. Acad. Sci. U.S.A.* **101**, 3118–3123.
- Manikkam, M., Tracey, R., Guerrero-Bosagna, C. and Skinner, M. K. (2012). Dioxin (TCDD) induces epigenetic transgenerational inheritance of adult onset disease and sperm epimutations. *PLoS One* **7**, 1–15.
- Martinez, J. M., DeVito, M. J., Birnbaum, L. S. and Walker, N. J. (2003). Toxicology of dioxin and dioxin-like compounds. In *Dioxins and Health*, 2nd ed. (A. Schecter and T. Gasiewicz Eds.), pp. 137–157. John Wiley & Sons, Inc, Hoboken, NJ.
- Mathew, L. K., Sengupta, S. S., Ladu, J., Andreasen, E. A. and Tanguay, R. L. (2008). Crosstalk between AHR and Wnt signaling through R-Spondin1 impairs tissue regeneration in zebrafish. *FASEB J.* **22**, 3087–3096.
- Mazieres, J., You, L., He, B., Xu, Z., Lee, A. Y., Mikami, I., McCormick, F. and Jablons, D. M. (2005). Inhibition of Wnt16 in human acute lymphoblastoid leukemia cells containing the t(1;19) translocation induces apoptosis. *Oncogene* **24**, 5396–5400.
- Mehta, V., Ablner, L. L., Keil, K. P., Schmitz, C. T., Joshi, P. S. and Vezina, C. M. (2011). Atlas of Wnt and R-spondin gene expression in the developing male mouse lower urogenital tract. *Dev. Dyn.* **240**, 2548–2560.
- Mehta, V., Schmitz, C. T., Keil, K. P., Joshi, P. S., Ablner, L. L., Lin, T. M., Taketo, M. M., Sun, X. and Vezina, C. M. (2013). Beta-catenin (CTNNB1) induces Bmp expression in urogenital sinus epithelium and participates in prostatic bud initiation and patterning. *Dev. Biol.* **376**, 125–135.
- Nishita, M., Enomoto, M., Yamagata, K. and Minami, Y. (2010). Cell/tissue-tropic functions of Wnt5a signaling in normal

- and cancer cells. *Trends Cell Biol.* **20**, 346–354.
- Nygren, M. K., Døsen-Dahl, G., Stubberud, H., Wälchli, S., Munthe, E. and Rian, E. (2009). β -catenin is involved in N-cadherin-dependent adhesion, but not in canonical Wnt signaling in E2A-PBX1-positive B acute lymphoblastic leukemia cells. *Exp. Hematol.* **37**, 225–233.
- Procházková, J., Kabátková, M., Bryja, V., Umannová, L., Bernatík, O., Kozubík, A., Machala, M. and Vondráček, J. (2011). The interplay of the aryl hydrocarbon receptor and beta-catenin alters both AhR-dependent transcription and Wnt/beta-catenin signaling in liver progenitors. *Toxicol. Sci.* **122**, 349–360.
- Simons, B. W., Hurley, P. J., Huang, Z., Ross, A. E., Miller, R., Marchionni, L., Berman, D. M. and Schaeffer, E. M. (2012). Wnt signaling through beta-catenin is required for prostate lineage specification. *Dev. Biol.* **371**, 246–255.
- Sulentic, C. E. W. and Kaminski, N. E. (2011). The long winding road toward understanding the molecular mechanisms for B-cell suppression by 2,3,7,8-tetrachlorodibenzo-*p*-dioxin. *Toxicol. Sci.* **120**(Suppl. 1), S171–S191.
- Sun, Y., Campisi, J., Higano, C., Beer, T. M., Porter, P., Coleman, I., True, L. and Nelson, P. S. (2012). Treatment-induced damage to the tumor microenvironment promotes prostate cancer therapy resistance through WNT16B. *Nat. Med.* **18**, 1359–1368.
- Teh, M.-T., Blaydon, D., Ghall, L. R., Briggs, V., Edmunds, S., Pantazi, E., Barnes, M. R., Leigh, I. M., Kelsell, D. P. and Philpott, M. P. (2007). Role for WNT16B in human epidermal keratinocyte proliferation and differentiation. *J. Cell Sci.* **120**, 330–339.
- Thomson, A. A. (2008). Mesenchymal mechanisms in prostate organogenesis. *Differentiation* **76**, 587–598.
- Tian, Y. (2009). Ah receptor and NF- κ B interplay on the stage of epigenome. *Biochem. Pharmacol.* **77**, 670–680.
- Vezina, C. M., Allgeier, S. H., Moore, R. W., Lin, T. M., Bemis, J. C., Hardin, H. A., Gasiewicz, T. A. and Peterson, R. E. (2008). Dioxin causes ventral prostate agenesis by disrupting dorsoventral patterning in developing mouse prostate. *Toxicol. Sci.* **106**, 488–496.
- Vezina, C. M., Hardin, H. A., Moore, R. W., Allgeier, S. H. and Peterson, R. E. (2010). 2,3,7,8-Tetrachlorodibenzo-*p*-dioxin inhibits fibroblast growth factor 10-induced prostatic bud formation in mouse urogenital sinus. *Toxicol. Sci.* **113**, 198–206.
- Vezina, C. M., Lin, T.-M. and Peterson, R. E. (2009). AHR signaling in prostate growth, morphogenesis, and disease. *Biochem. Pharmacol.* **77**, 566–576.
- Yamada, W., Nagao, K., Horikoshi, K., Fujikura, A., Ikeda, E., Inagaki, Y., Kakitani, M., Tomizuka, K., Miyazaki, H., Suda, T., et al. (2009). Craniofacial malformation in R-spondin2 knockout mice. *Biochem. Biophys. Res. Commun.* **381**, 453–458.
- Zhang, T. J., Hoffman, B. G., Ruiz de Algora, T. and Helgason, C. D. (2006). SAGE reveals expression of Wnt signalling pathway members during mouse prostate development. *Gene Expr. Patterns* **6**, 310–324.